

# Borophene: New Sensation in Flatland

Pranay Ranjan, Jang Mee Lee, Prashant Kumar,\* and Ajayan Vinu\*

Borophene, a 2D allotrope of boron and the lightest elemental Dirac material, is the latest very promising 2D material owing to its unique structural and electronic characteristics of the  $X_3$  and  $\beta_{12}$  phases. The high atomic density on ridgelines of the  $\beta_{12}$  phase of borophene provides a substantial orbital overlap, which leads to an excellent electron density in the conduction level and thus to a highly metallic behavior. These unique structural characteristics and electronic properties of borophene attract significant scientific interest. Herein, approaches for crystal growth/synthesis of these unique nanostructures and their potential technological applications are discussed. Various substrate-supported ultrahigh-vacuum growth techniques for borophene, such as molecular beam epitaxy, atomic layer deposition, and chemical vapor deposition, along with their challenges, are also summarized. The sonochemical exfoliation and modified Hummer's technique for the synthesis of free-standing borophene are also discussed. Solution-phase exfoliation seems to address the scalability issues and expands the applications of these unique materials to various fields, including renewable energy devices and ultrafast sensors. Furthermore, the electronic, optical, thermal, and elastic properties of borophene are thoroughly discussed and are compared with those of graphene and its "cousins." Numerous frontline applications are envisaged and an outlook is presented.

Hall effects but also several exotic behaviors including high-temperature superconductivity.<sup>[1]</sup> Numerous frontier technologies such as ultrafast thermal imaging for night-vision cameras, prompt diabetic testing, laser shielding, defense (body armor), smart electronic cooling solutions, flexible digital electronics, and hybrid energy storage have been realized using 2D materials.<sup>[2]</sup> Notably, applications are being invented every other day.<sup>[3]</sup> Since the invention of graphene by Geim and Novoselov, numerous 2D materials have been discovered and added to the family of 2D nanostructures. They can primarily be classified as elemental, oxides, nitrides, dichalcogenides, compounds, and complex oxides.<sup>[4]</sup>

Graphene, the first member of the "flatland" materials, has paved the way for the development of innovative technologies addressing industrial problems. It also enables a significant progress in the development of nanotechnology devices for various applications including sensors and energy storage and conversion.

## 1. Introduction

2D materials have attracted considerable scientific interest as they exhibit not only extreme carrier mobilities and quantum


Recently, 2D-Xenes have been experimentally envisaged as new "cousins" of graphene and also as new members of the flatland family.<sup>[4c,i]</sup> Unlike graphene, which has an  $sp^2$  hybridization ( $\pi$  bonds) without dangling bonds, Xenes have mixed  $sp^2$ – $sp^3$  hybridizations and require substrates to saturate the (out-of-plane) dangling bonds. The bondings between the layers in Xenes are attributed to electron–electron correlations. Xenes ( $X = \text{Si, Ge, Sn, etc.}$ ) are also known as pseudoplanar 2D materials, such as silicene, germanene, stanene, plumbene, phosphorene, and borophene, with group III to IV elements.<sup>[4j,n]</sup> They generally offer more extensive ranges for covalent functionalization owing to their buckled structures. The buckling is deemed to foster numerous futuristic engineered devices and thus Xenes are regarded as next-generation materials in electronic industries.<sup>[4]</sup> Borophene, the newest member in the Xene family and lightest elemental Dirac material with a single layer of boron, is very promising owing to its unique electronic, superconductive, elastic, thermal, anisotropic mechanical, optical, and transport properties. These properties are suitable for several advanced technological applications, such as energy storage, gas sensing, and catalysis.<sup>[5]</sup> Among the numerous allotropes of borophene, considered metallic, few of the borophene phases have been synthesized, including the honeycomb,  $X_3$ ,  $\beta_{12}$ , and 2- $Pmmn$  phases, considered metallic. As a new 2D material, borophene attracts increasing interest in the stiff competition against the related contemporary materials including

Dr. P. Ranjan, Prof. P. Kumar  
 Department of Physics  
 Indian Institute of Technology Patna  
 Bihta, Patna, Bihar 801103, India  
 E-mail: prashantkumar@iitp.ac.in

Dr. P. Ranjan  
 Department of Physics  
 UAE University  
 Al-Ain, Abu Dhabi 15551, United Arab Emirates

Dr. J. M. Lee, Prof. A. Vinu  
 Global Innovative Centre for Advanced Nanomaterials  
 School of Engineering  
 Faculty of Engineering and Built Environment  
 The University of Newcastle  
 Callaghan, NSW 2308, Australia  
 E-mail: Ajayan.Vinu@newcastle.edu.au

Prof. P. Kumar  
 Birck Nanotechnology Centre  
 Purdue University  
 West Lafayette, IN 47907, USA

 The ORCID identification number(s) for the author(s) of this article can be found under <https://doi.org/10.1002/adma.202000531>.

DOI: 10.1002/adma.202000531

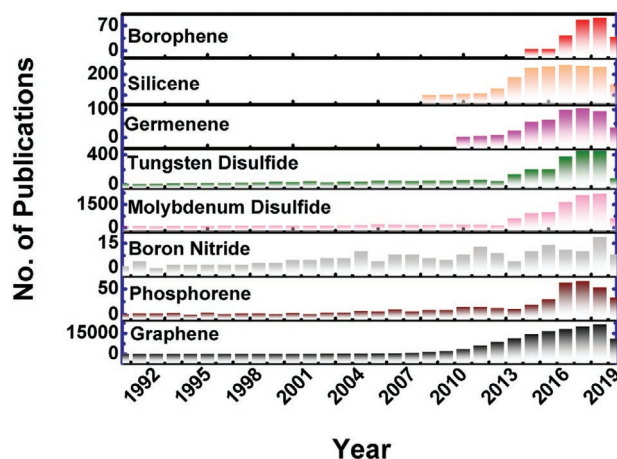


**Figure 1.** The number of publications per year on various 2D materials (graphene, phosphorene, boron nitride, transition metal dichalcogenides, germanene, silicone, and borophene).

graphene, boron nitride (BN), phosphorene, transition-metal dichalcogenides (TMDCs), and germanene (Figure 1).<sup>[5a,6]</sup> Among the series of unique 2D materials, borophene has attracted considerable attention owing to its unique chemical structure and impressive electronic conductivity and surface properties. Apart from the usual covalent bonding, boron can form a three-center two-electron bonding,<sup>[7]</sup> which enables the formation of a considerable number of atomic clusters having various sizes and atomic bindings (Figure 2).<sup>[8]</sup> Graphene, the first discovered 2D material, is semimetallic, phosphorene is semiconducting, while borophene is metallic (Figure 3).<sup>[9]</sup> Graphene exhibits an electron-hole symmetry with the Fermi level in the middle between the valence and conduction bands. The electron band structure of borophene differs from that of graphene (Figure 4). The unique electronic structure of borophene inspires studies on its electronic, thermal, optical, and optoelectronic behaviors.

The characteristic structure of borophene makes it an attractive material. For example, the electron-deficient p orbital in

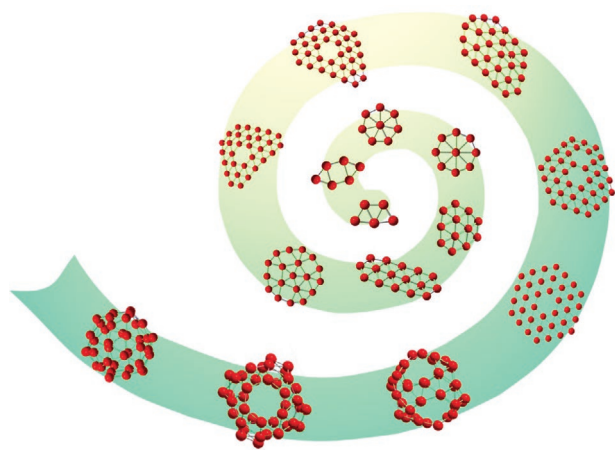


**Figure 2.** Allotropes of boron clusters. First 12 images from the center of the spiral: Reproduced with permission.<sup>[8a]</sup> Copyright 2019, Royal Society of Chemistry. Last three images, at open end of spiral: Reproduced with permission.<sup>[8b]</sup> Copyright Prof. Lai-Sheng Wang, Department of Chemistry, Brown University, Providence, RI, USA.



**Prashant Kumar** received his doctorate in physics in April 2009 from the University of Hyderabad, and worked with Prof. C. N. R. Rao at JNCASR Bangalore as a DST Nanoscience Postdoc till June 2012. He then worked as a Raytheon-funded Postdoc with Prof. Timothy S. Fisher at Purdue University, USA. From April 2013 onward, he worked

as an NSF-funded Postdoc with Prof. Gary J. Cheng at Purdue University. Being awarded a Ramanujan Fellowship, he started working at the Indian Institute of Technology Patna in June 2015. His research interests include novel synthetic strategies for 2D materials, their hybrids, and doped nanosystems with emphasis on energy solutions.



**Ajayan Vinu** is Global Innovation Chair Professor and the Director of Global Innovative Centre for Advanced Nanomaterials at the University of Newcastle. During his 20 years of research, he has made a tremendous contribution in the field of nanoporous materials, 2D nanomaterials, nanoparticles, and their application in

sensing, energy storage, fuel cells, adsorption and separation, and catalysis.

boron leads to its vivid structural landscape, complex allotropic structures, and superior topological and physical properties, which make borophene a unique material. Boron has two electrons in its s shell and one electron in its outer shell (p shell ( $2s^2 2p^1$ )). Moreover, the electron-deficient boron outer orbital provides two- and three-center bondings and is considered crucial in the bonding mechanisms, which eventually lead to protrusion and defects in sheets and complex bondings. The in-plane bonding ( $\sigma$  and  $\sigma^*$  bondings) in boron sheets

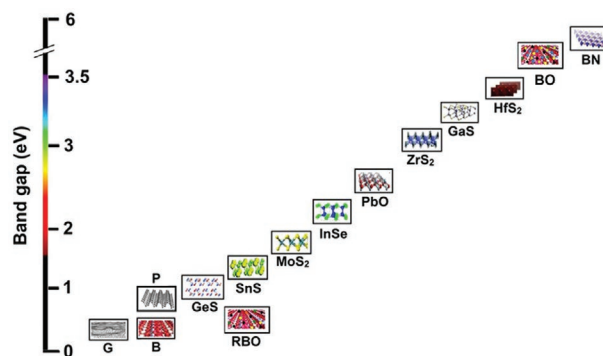


**Figure 3.** The family of 2D materials.

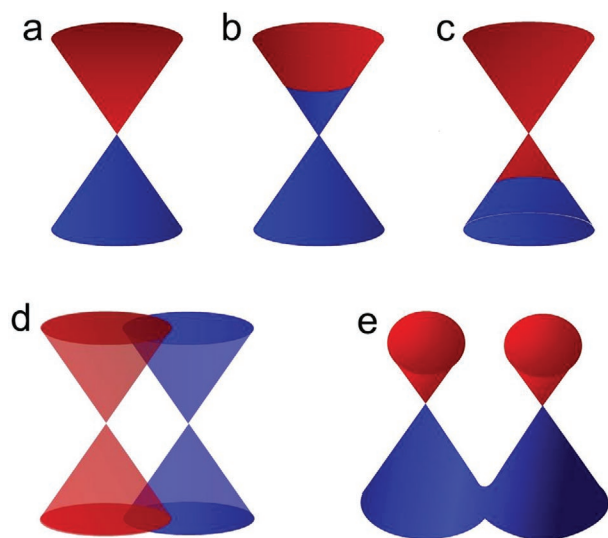


**Figure 4.** a–e) Dirac cones of graphene (a), n-doped graphene (b), p-doped graphene (c), phosphorene (d), and borophene (e).

(triangular boron,  $\beta_{12}$ , and  $X_3$ ) is attributed to the collective contribution of  $s$ ,  $p_x$ , and  $p_y$  orbitals, whereas the out-of-plane bonding ( $\pi$  and  $\pi^*$  bondings) is attributed to  $p_z$  orbitals.<sup>[9c]</sup>

The electronic mobility depends on several factors, including the atomic number (available electrons), atomic size, atom valence, crystal structure, chemical bondings between the atoms, and strain in the system. Thus, it exhibits a strong material dependence. It has been predicted that graphene has an electronic mobility as high as  $180\,000\text{ cm}^2\text{ V}^{-1}\text{ s}^{-1}$ ,<sup>[10]</sup> which is perhaps the highest value among 2D materials. Its “cousins” silicene ( $2100\text{ cm}^2\text{ V}^{-1}\text{ s}^{-1}$ ),<sup>[11]</sup> germanene ( $2800\text{ cm}^2\text{ V}^{-1}\text{ s}^{-1}$ ),<sup>[11]</sup> stanene ( $3000\text{ cm}^2\text{ V}^{-1}\text{ s}^{-1}$ ),<sup>[11]</sup> and phosphorene ( $1000\text{ cm}^2\text{ V}^{-1}\text{ s}^{-1}$ )<sup>[12]</sup> have moderate mobilities. In contrast, the semiconducting molybdenum diselenide ( $50\text{ cm}^2\text{ V}^{-1}\text{ s}^{-1}$ ), tungsten diselenide ( $180\text{ cm}^2\text{ V}^{-1}\text{ s}^{-1}$ ), molybdenum disulfide ( $200\text{ cm}^2\text{ V}^{-1}\text{ s}^{-1}$ ), and tungsten disulfide ( $0.2\text{ cm}^2\text{ V}^{-1}\text{ s}^{-1}$ )<sup>[13]</sup> have lower mobilities. BN, an insulator, has even worse mobility,  $0.05\text{ cm}^2\text{ V}^{-1}\text{ s}^{-1}$ . Notably, it has been predicted that borophene has a mobility as high as  $280\,000\text{ cm}^2\text{ V}^{-1}\text{ s}^{-1}$ ,<sup>[14]</sup> even higher (along ridgeline) than that of graphene. This unique property makes it promising. It inspires analyses of its structure and applications in various fields, including energy storage and sensing.

Mannix et al.<sup>[15]</sup> have reported that the phonon dispersion of a free-standing borophene sheet varies owing to the structural anisotropy. Near the  $\Gamma$ -point, the small imaginary frequencies are consistent, while long-wavelength transverse waves are unstable and can be fixed with defects, protrusion, or grain boundaries. Thus, the thermal conductivity of borophene (anisotropic material) must be low in comparison to those of other isotropic 2D materials. Among the 2D materials, graphene exhibits a superior thermal conductivity of  $3846\text{ W m}^{-1}\text{ K}^{-1}$ , followed by that of BN of  $1055\text{ W m}^{-1}\text{ K}^{-1}$ . The thermal conductivity of borophene is  $233.3\text{ W m}^{-1}\text{ K}^{-1}$ , which seems to be the next value to that of BN (third in the list). The thermal conductivities of other 2D materials, such as stanene, silicene, germanene,  $\text{MoS}_2$ , and phosphorene are 2.9, 9.4, 9.87, 103.4, and  $180\text{ W m}^{-1}\text{ K}^{-1}$ , respectively.<sup>[16]</sup>

As stated above, borophene is the lightest elemental Dirac metallic material with a negligible spin–orbit coupling,<sup>[17]</sup> unlike graphene and other 2D materials having strong spin–orbit couplings. Recent theories based on simulations show that borophene is partially ionic with double Dirac cones near the Fermi level.<sup>[18]</sup> Striped borophene sheets have tilted semi-Dirac cones.<sup>[19]</sup> Recently, through a tight-binding analysis, Feng et al.<sup>[20]</sup> have proposed that the  $\beta_{12}$  phase of a borophene sheet onto a Ag (111) surface can be decomposed into two triangular sublattices. In a similar manner, the honeycomb lattice can exhibit Dirac cones. Moreover, the same group<sup>[20]</sup> has introduced a periodic perturbation theory and observed that the Dirac cones are split. This hypothesis was confirmed by angle-resolved photoemission spectroscopy and first-principle calculations. This demonstrates the potentials of borophene-sheet-based futuristic electronic devices for the realization of novel high-speed low-power electronic devices. Mannix et al.<sup>[15]</sup> have carried out a density functional theory (DFT) calculation to predict the band structure of a monolayer atomic free-standing  $X_3$  borophene sheet within the 2D Brillouin zone (unstrained relaxed borophene atomic sheets). They have reported that the electronic bands of the borophene monolayer sheets overlap each other at the Fermi level, which yields the metallic structure. Moreover, the protrusion (out-of-plane oriented atoms) in the  $\beta_{12}$  phase opens up a bandgap and creates an anisotropy. This structural anisotropy creates a considerable mechanical anisotropy owing to the strong B–B bond (protrusion), which leads to unique properties, such as expansion of the sheets (in-plane) under a tensile strain.

By DFT calculations, the same group has also demonstrated that if the structural anisotropy by the protrusion is relaxed, the corrugation in a particular direction would decrease, which would lead to a decreased unit cell size. Mannix et al.<sup>[15]</sup> have calculated the in-plane Young’s moduli of a free-standing borophene sheet ( $\approx 170$  and  $\approx 398\text{ GPa}$  along the two directions), high in comparison to that of a graphene sheet ( $340\text{ GPa}$ ). Through their seminal studies, Mortazavi et al., Wang et al., Le et al., Zhou and Jiang, and Yi et al.<sup>[21]</sup> have predicted that free-standing borophene sheets are vulnerable for environmental degradation (due to defects, functionalization, hydrogen bonding, structural phase transition, and temperature variations) and hence a lower Young’s modulus is expected. The Young’s moduli of borophene and other 2D materials are compared in Figure 9, discussed below. The Young’s moduli of various 2D materials including germanene ( $42.7, 42.7\text{ GPa}$ ), silicene ( $60.6, 60.6\text{ GPa}$ ),  $\text{MoS}_2$  ( $125, 123\text{ GPa}$ ), boron nanoribbon ( $127.12, 127.12\text{ GPa}$ ), BN ( $275.8, 275.8\text{ GPa}$ ), graphene ( $338.08, 338.08\text{ GPa}$ ), phosphorene ( $167.88, 39.39\text{ GPa}$ ), borophene (triangular,  $399, 398\text{ GPa}$ ), and borophene ( $398, 170\text{ GPa}$ )<sup>[15,21c,22]</sup> have been obtained by DFT calculations in the  $Y_a$  and  $Y_b$  directions, respectively.

Considering the unique borophene electron-deficient bonds apart from the usual binding, it is of interest to analyze the binding and equilibrium atomic structures. Eigen-structures are prevalent in 2D materials. Therefore, studies on the impacts of atomic configurations in the sheet on various physical and chemical properties would provide a new platform for the development of devices and sensors.

Borophene has two planar atomic sheet configurations.<sup>[23]</sup> One of them is perfectly flat, referred to as  $X_3$  phase, while  $\beta_{12}$



is an atomic sheet having atomic ridges. Such ridges provide higher electron densities along them.<sup>[24]</sup> The spaces between the ridgelines can act as channels for ion transport in energy storage applications. The atomic binding of gaseous molecules on a borophene surface is expected to be better on the ridgeline as it can provide an enhanced anchoring. Similarly, increased catalytic activities are expected. The unique properties and high potential for technological applications make borophene a promising material. However, further studies on its structural characteristics and properties are required before it can be commercialized.

Recently, a few review articles on the fabrication and applications of borophene have been reported.<sup>[5d,f]</sup> They are focused mainly on the ultrahigh-vacuum deposition of borophene by atomic layer deposition (ALD) and molecular beam epitaxy (MBE). These methods limit large-scale applications of materials where grams and kilograms of free-standing materials are needed. In this review, we summarize the progress of borophene from its emergence to recent developments, which promise a scalable synthesis of borophene, and applications and propose future endeavors. We consider two prominent phases,  $\beta_{12}$  and  $X_3$ , which are incidentally metallic. The metallic structure (particularly the free electrons) is needed for sensing in addition to the electronic mobility, a well-known characteristic of the 2D materials. The electronic, photonic, thermal, and thermoelectric sensing of various gases and small molecules (possibly viruses in the future) by borophene, which would primarily depend on its electronic structure, are described in this review. The new developments in the synthesis of borophene with different phases by controlling the solvents are described. In particular, the binding chemistry and cluster formation in borophene are analyzed to elucidate the origin making particular phases favorable. Various physical properties such as the thermal, optical, mechanical, electrical, and elastic properties and mobility of borophene are compared to those of other 2D materials. A comparative analysis of borophene against graphene, boron nitride, TMDCs, and MXene is presented. This review could guide large-scale applications in the energy sector, catalysis, green chemistry, nanocomposites, nanohybrids, heterolayered devices, and sensors. Finally, an outlook on borophene is presented considering its important role in material science and applications.

## 2. Substrate-Supported Crystal Growth

### 2.1. ALD

The first synthesis of borophene was carried out by Mannix et al.<sup>[15]</sup> in 2015 by ALD (rate: 0.01–0.1 monolayer  $\text{min}^{-1}$ ; accelerating voltage: 1.8–2.3 kV; filament current: 1.5–1.9 A; pressure:  $<0.5 \times 10^{-10}$  mbar) on a Ag(111) surface. They have fabricated borophene sheets whose crystal growth was catalyzed by the silver substrate.<sup>[15]</sup> The same group have also observed  $\beta_{12}$  (corrugated “striped” phase) and  $X_3$  (homogeneous phase) anisotropic phases of borophene at different increased temperatures (450 and 700 °C, respectively). A high deposition temperature and low deposition rate lead to the formation of a stable striped phase. A low temperature and high rate of deposition favor the metastable phase. The phase purity and absence of impurities/compounds

and alloys were confirmed by X-ray photoelectron spectroscopy, while the structural anisotropies such as the periodic vertical buckling, short-range rhombohedral Moiré pattern, and longer-range 1D Moiré pattern were confirmed by atomic force microscopy and high-resolution transmission electron microscopy. An analysis of the microscopic images (low-energy electron diffraction) has demonstrated that the  $\beta_{12}$  and  $X_3$  phases exhibit a threefold orientation degeneracy with respect to the substrate.

### 2.2. MBE

In 2016, the 2D structure of borophene was confirmed by Feng et al.<sup>[25]</sup> by growing borophene atomic sheets on Ag(111) at temperatures of 550–800 K by MBE (the pressure during the boron growth was  $6 \times 10^{-10}$  Torr). A pure boron (99.9999%) was evaporated onto a clean Ag(111) substrate. The single-crystal Ag(111) was cleaned by repeated argon ion sputtering with a boron flux of  $\approx 0.1$  monolayer  $\text{min}^{-1}$ . Feng et al.<sup>[25]</sup> and Mannix et al.<sup>[15]</sup> have observed the formation of  $\beta_{12}$  and  $X_3$  phases. Their close observations of the atomic structures have revealed that the densities of boron atoms in the two phases are distinguishable, though the difference is small, despite the use of different deposition techniques. The growths of borophene by ALD and MBE fundamentally limit the borophene deposition to small areas, which makes the fabrication of practical devices at an industrial scale challenging and costly.

### 2.3. Chemical Vapor Deposition (CVD)

CVD enables the syntheses of various 2D materials on an industrial scale. CVD has attracted considerable attention considering its incumbency in the industry and recently reported ability to grow very-large-scale graphene sheets. Tai et al.<sup>[6f]</sup> for the first time, have successfully grown a borophene-like material on Cu by CVD at 1100 °C and B:B<sub>2</sub>O<sub>3</sub> ratio of 1:1, similar to those used in the graphene synthesis. However, the synthesized material was primarily multilayered and consisted of the common  $\gamma$ -phase. The merit of the vacuum-grown (by MBE/ALD/CVD) borophene is its chemical purity crucial for its characteristic physical and chemical behaviors. The depositions of borophene sheets have been realized by ALD and MBE. Tai et al.<sup>[6f]</sup> have proposed a method for the growth of a thick borophene-like structure on a copper substrate, which has not provided borophene islands. Wu et al.<sup>[26]</sup> have proposed a modified considerably improved technique for a CVD growth of monolayer borophene sheets having micrometer sizes on thick Cu(111) films grown on sapphire. This further advances the borophene-based devices and paves the way for the realization of corresponding electronic devices.

The provision of ultrahigh-vacuum experimental conditions in laboratories is challenging and very costly. Moreover, it has been suggested by the pioneers that the use of a catalyst is important to enhance the crystallization.<sup>[27]</sup> Thus, it has been wrongly believed that borophene could not be grown without substrate. This hypothesis of elusive growth has prevented researchers from analyses in a scalable manner and thus its potential applications have not been demonstrated.

### 3. Realization of Free-Standing Borophene

#### 3.1. Sonochemical Exfoliation

The synthesis of borophene is quite challenging as it usually requires highly sophisticated fabrication facilities and ultralow pressures. Even with such facilities, it is challenging to obtain defect-free borophene nanosheets. In general, a sonochemical synthesis would yield a monolayer, bilayer, trilayer, and quadruple layer depending on the sonication time and solvent type. If the solvent interacts correctly, it helps achieve monolayer sheets with large lateral dimensions. If it does not interact well, it yields sheets with a large number of stacking layers upon sonication for the same time, while a prolonged sonication would lead to fragmentation leading to tiny sheets (borophene dots). Therefore, the choice of an adequate solvent and optimization of the sonication time are essential for a larger-dimension exfoliation of borophene sheets.

The exfoliation of borophene can be explained through the liquid-phase exfoliation of 2D materials, as illustrated by Coleman and others.<sup>[28,29]</sup> The enthalpy of mixing of borophene in a solvent and electrostatic charge transfer between the atomic sheets of borophene and solvent molecules (such as isopropyl alcohol, deionized water, acetone, ethylene glycol, and dimethylformamide) determine the miscibility of the sheets and thus its liquid-phase exfoliation.

The thermodynamic equation for the mixing of sheets in solvents is

$$\Delta H_{\text{mix}}/V_{\text{mix}} \approx 2/T_B \left( (E_{\text{S,S}})^{1/2} - (E_{\text{S,B}})^{1/2} \right)^2 \phi_B \quad (1)$$

where  $\Delta H_{\text{mix}}$  and  $V_{\text{mix}}$  are the enthalpy of mixing and mixture volume, respectively,  $T_B$  is the thickness of the borophene nanosheet,  $E_{\text{S,S}}$  and  $E_{\text{S,B}}$  are the surface energies of the solvent and borophene, respectively, and  $\phi_B$  is the volume fraction of the dispersed borophene sheets. Thus,  $\Delta H_{\text{mix}}$  would have the minimum value if  $E_{\text{S,S}}$  and  $E_{\text{S,B}}$  are similar. In such case, a minimal external sonication energy is required for exfoliation. The free-standing borophene sheet seems to form upon a reflex action originating out of the lattice. The local strain development and its relaxation are the origins for the formation of such structures. The interaction of the solvent with the borophene sheet is crucial in the exfoliation into the monolayer. Indeed, in the sonochemical exfoliation, acetone has yielded a monolayer formation in our experimental trial. In contrast, successful exfoliation could not be achieved with other solvents, which confirms that the atomic interactions between the solvent and surface of the sheet to be exfoliated are important in the liquid-phase exfoliation.

#### 3.2. Modified Hummer's Approach

The next challenge, overcome by Ranjan et al.,<sup>[29a]</sup> was to obtain large-scale free-standing borophene sheets in a scalable manner. Ranjan et al.<sup>[29a]</sup> have used improved modified Hummer's techniques and demonstrated the significant role of the ratio of boron and potassium permanganate on the exfoliation. Before their study, the experimental realization of borophene has been very limited to a substrate-supported growth (Figure 5).



**Figure 5.** Synthesis procedure for 2D borophene atomic sheets.<sup>[6f,15,25,29a]</sup>

The recent experimental study by Ranjan et al.<sup>[29a]</sup> on the synthesis of free-standing borophene atomic sheets through the combination of the modified Hummer's technique (chemical exfoliation) and sonochemical exfoliation has largely advanced the field of borophene synthesis. It is the first synthesis of pure crystalline large-area free-standing borophene sheets with applications in sensing of gas, molecules (surface-enhanced Raman spectroscopy (SERS)-based), and strain. They have also analyzed the role of the solvent on the borophene atomic structures synthesized through sonochemical exfoliation. The modified Hummer's method has yielded borophene oxide, which has been subsequently reduced. The chemical synthesis could provide a scalable synthesis of free-standing borophene sheets for several applications. The hypothesis that free-standing borophene could not exist was finally disproved by Ranjan et al.,<sup>[29a]</sup> which has been widely accepted in the scientific community. In this seminal study, the existence of  $\beta_{12}$  and  $X_3$  phases was confirmed in addition to an intermediate phase. It was also shown that the phase evolution was strain-driven. Their study is still the only experimental study on the isolation and device formation of free-standing borophene. The scalable synthesis of free-standing borophene not only disproves the hypothesis that the free-standing borophene could not exist but also shows that the  $\beta_{12}$ ,  $X_3$ , and their intermediate phases form in a single chemical reaction. The number of layers, interlayer interactions, and strain are critical factors governing the phase formation.<sup>[29a]</sup> An outlook comparing the free-standing borophene to those obtained by MBE, ALD, and CVD<sup>[15,25,29a]</sup> is shown in Figure 6.

### 4. Unique Properties of Borophene

#### 4.1. Electronic Properties

Boron has different polymorphs (5–16) owing to the electron deficiency. However, the structural frustration at the atomic level in borophene has been less investigated, compared to its bulk counterpart. The  $\beta_{12}$  and  $X_3$  phases of borophene sheets are stable and metallic in contrast to the hexagonal and

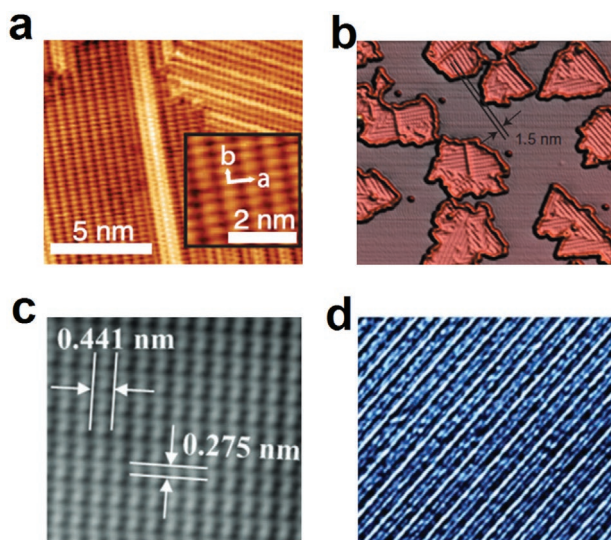


**Figure 6.** a,b,d)  $\beta_{12}$  phase of borophene obtained by Mannix et al.<sup>[15]</sup> (a), Feng et al.<sup>[25]</sup> (b), and Ranjan et al.<sup>[28a]</sup> (d), and c)  $\gamma$ -phase by Tai et al.<sup>[6f]</sup> a) Reproduced with permission.<sup>[15]</sup> Copyright 2015, AAAS. b) Reproduced with permission.<sup>[25]</sup> Copyright 2016, Springer Nature. c) Reproduced with permission.<sup>[6f]</sup> Copyright 2015, Wiley-VCH. d) Reproduced with permission.<sup>[28a]</sup> Copyright 2019, Wiley-VCH.

triangular lattice structures of borophene. The instability of the boron sheets (e.g., the hexagonal lattice structure (metallic and acceptor) of borophene) is attributed to the half-filled  $\pi$  bonding as well as the incomplete three  $\sigma$  bondings. However, in the flat triangular lattice (metallic and donor), the overoccupied  $\sigma^*$ -bonding states were considered as the origin of the instability. The Fermi level of the triangular lattice would be above the bonding and antibonding states. Thus, it was predicted (in an ideal case) that a mixed state with the hexagon lattice exists and that the triangular lattice is the most stable state and metallic.<sup>[9c]</sup>

## 4.2. Optical Properties

The anisotropic atomic arrangement, particularly the ridgeline in the  $\beta_{12}$  phase of borophene, has attracted considerable interest, as the high atomic density would lead to enhanced atomic interactions and stronger chemical bonding, and thus to improved electronic mobility, thermal conductivity, energy storage, gas sensing, catalysis, and elastic modulus.<sup>[10–16m-p,21,22,30]</sup> The bandgap and electronic mobility of borophene are compared to those of other 2D materials in **Figure 7**. For an ideal Dirac fermion system (infinite lattice without defects), the transmission for a monolayer should be smaller than 100% by  $\pi\alpha$  ( $3.14/137 \approx 2.3\%$ ), where  $\alpha$  is the fine structure coefficient, i.e., 97.7%. However in 2D materials, such as borophene, edge defects, and localized 3D atomic protrusion are unavoidable, which would enhance the absorption at higher energies (in the blue, violet, or even ultraviolet ranges) without affecting the larger-wavelength transmission (97.7%).<sup>[31]</sup> For an  $N$ -layered borophene, it would be  $(100 - N\pi\alpha)$ . However, this formula neglects the interlayer interactions. In real systems, such interactions occur owing to the inevitable orbital hybridizations, which increases the transmission. As explained by Ranjan et al.,<sup>[29]</sup> the full width at half maximum and absorption of the

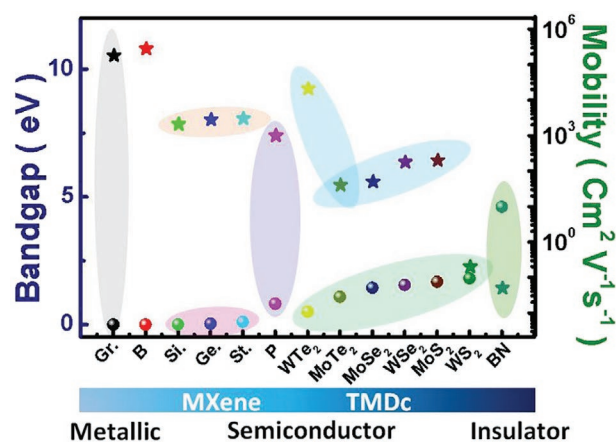


**Figure 7.** Bandgap versus mobility of various 2D materials.

dispersion are larger at a low centrifugation speed (which is expected to yield a dispersion with a considerable variation in number of sheets). This result obtained by Ranjan et al.<sup>[29a]</sup> is consistent with the results for graphene reported by the Novoselov's group and is quite unusual for the case of an anisotropic material.

## 4.3. Mechanical and Thermal Properties

Ranjan et al.<sup>[29a]</sup> have experimentally demonstrated free-standing borophene sheets and analyzed their mechanical strength in a borophene nanocomposite with poly(vinylidene difluoride). A free-standing borophene sheet (nanofiller) content of 1% has provided the best results for elongation. It was theoretically predicted that the pristine borophene sheets exhibit high in-plane Young's moduli and Poisson's ratio anisotropy owing to the B–B bonds.<sup>[15]</sup> This unique structure of boron provides superior mechanical properties to those of other 2D materials. By a first-principles calculation, Zhang et al.<sup>[24b]</sup> have demonstrated that the bending stiffness of borophene sheets (concentration of hollow hexagons: 1/6) is two times that of graphene. Moreover, under tension, they have observed that the delocalized multicenter chemical bonding in borophene underwent structural phase transition before fracturing. Borophene sheets without H–H bonds are even stronger than graphene and are promising materials for advanced composites. At this stage, it is too early to discuss the fundamental properties of borophene without measurements. The number of studies related to theoretical calculations of mechanical properties of borophene exponentially increases. The reduced dimensionality, anisotropy, different polymorphs, and lateral size are few critical parameters of the borophene sheet determining its mechanical strength.

Borophene exhibits metallic behaviors of both  $\beta_{12}$  and  $X_3$  phases. However,  $\beta_{12}$  exhibits an increased electron mobility along the ridgelines. As the ridgelines would act as excellent anchors, it would be suitable for molecular sensing using an electrical signal. The single-layer graphene exhibits an excellent thermal conductivity, while BN, even though is an electrical insulator, also exhibits thermal conductivity.<sup>[32]</sup> MoS<sub>2</sub> and WS<sub>2</sub>



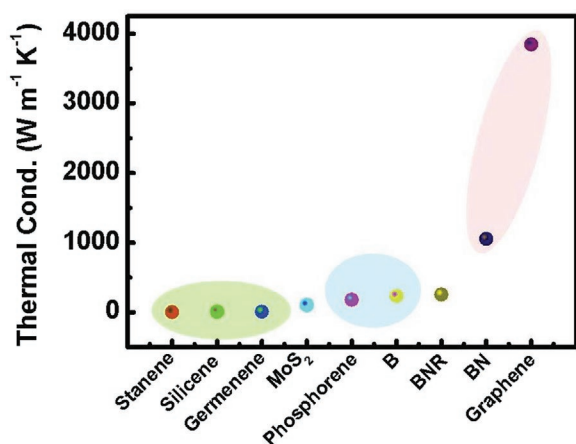


Figure 8. Thermal conductivity of various 2D materials.

are not good thermal conductors (Figure 8).<sup>[33]</sup> The atomic ridgelines in borophene are crucial and determine its elastic behavior. Thus, it exhibits the best Young's modulus among its counterparts (Figure 9). The  $\beta_{12}$  phase has two Young's moduli ( $\approx 170$  and  $\approx 398$  GPa), along the ridgeline and in the normal direction, respectively. Flat atomic sheets of borophene need to be produced in a scalable manner. Free-standing borophene sheets would facilitate the fabrication of devices for several applications. Applications of MBE- and ALD-grown borophene samples have not been demonstrated, while free-standing borophene has been successfully used for photosensing, gas sensing, SERS-based molecular sensing, and energy storage (Figure 10). The specific capacity of borophene oxide synthesized through the modified Hummer's route is very high ( $4941 \text{ mAh g}^{-1}$ ), compared to those of other 2D systems.

## 5. Potential Applications of Borophene

### 5.1. Gas Sensing

The properties of graphene suggest that 2D materials exhibit large surface areas and enhanced physical and chemical properties.

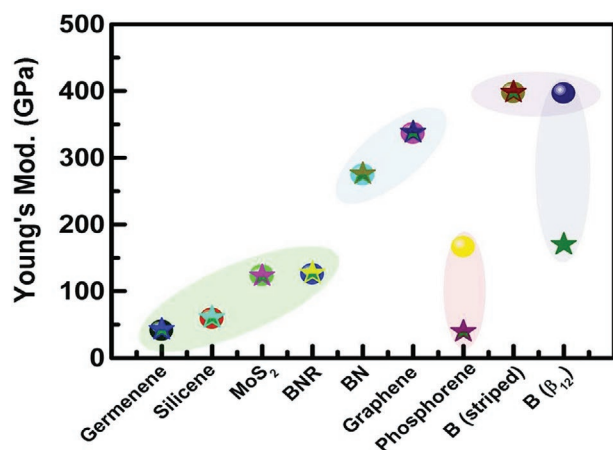


Figure 9. Young's modulus of various 2D materials.

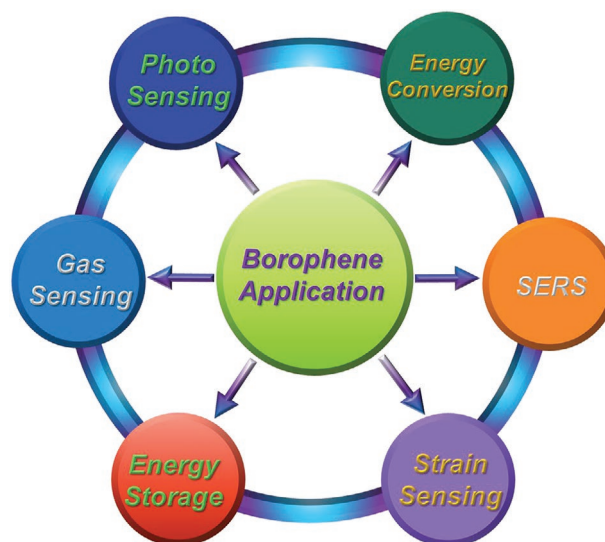


Figure 10. Applications of free-standing borophene atomic sheets.

The 2D materials (such as graphene, BN,  $\text{MoS}_2$ ,  $\text{WS}_2$ , and phosphorene) are promising candidates for futuristic nanodevice applications and thus have been investigated for sensing applications, owing to their high mobilities at monolayer thicknesses. However, materials such as graphene lack high sensitivity and selectivity, and thus cannot be used to detect toxic gases owing to the lack of electronic bandgap. The materials of the TMDC family, e.g.,  $\text{MoS}_2$ ,  $\text{MoSe}_2$ ,  $\text{WS}_2$ , and  $\text{WSe}_2$ , also exhibit low mobilities. These disadvantages have inspired studies on new 2D materials having mobilities higher than those of the TMDC family materials or almost equivalent to that of graphene. The successful use of graphene in molecular sensors (chemical and biological) is enabled by its electronic structure changes upon its interactions with molecules in its vicinity in addition to its record-high electronic mobility.

Borophene with the increased electronic density along ridgelines and metallic structure, which can provide electrons for chemical binding, is expected to exhibit a higher performance. It is of interest to evaluate its selectivity and sensing performance. One of the best real-time sensing applications of borophene has been reported by Ranjan et al.,<sup>[29a]</sup> where ammonia sensing has been performed on free-standing borophene sheets (Figure 10).

Borophene on different substrates has been extensively investigated through DFT calculations to understand the interactions, adsorptions, and sensing of toxic gases. Through theoretical calculations, Huang et al., Cui et al., Shukla et al., Liu et al., and Omidvar<sup>[34]</sup> have suggested that borophene is particularly suitable for sensing of toxic gases. Shukla et al.<sup>[34e]</sup> have analyzed the electronic and transport properties of monolayer borophene sheets through DFT calculations using the Vienna Ab initio Simulation Package (VASP27) within the generalized gradient approximation with the Perdew–Burke–Ernzerhof exchange–correlation functional. van der Waals corrections were implemented using the Grimme (DFT-D3) method upon adsorptions of CO, NO,  $\text{CO}_2$ ,  $\text{NO}_2$ , and  $\text{NH}_3$  gas molecules. The monolayer sheet of borophene has exhibited high binding energies for all gases but low binding energy for  $\text{CO}_2$  gas molecules.

Through a DFT calculation, Liu et al.<sup>[34c]</sup> have demonstrated that borophene sheets can act as electron donors. Therefore, any electron-acceptor molecule can easily interact with borophene, which can lead to chemical bonding. According to theoretical DFT calculations using the Cambridge Sequential Total-Energy Package (CASTEP) in Materials Studio 6.1,<sup>[34c]</sup> Liu et al. have reported that borophene is an excellent active material for sensing of CO<sub>2</sub> gas molecules.

## 5.2. Fuel Cells

Hydrogen-based futuristic fuel cells would provide clean energy and fuel efficiencies 2.5–2.7 times those of fossil fuels. However, the storage and transportation of hydrogen are challenging. A simple economical storage with high volumetric and gravimetric densities of hydrogen and long-term cyclic stability (reversibility) are desirable for hydrogen storage.<sup>[33a,d]</sup> Materials having high surface-area-to-volume ratios and binding energies of 0.20–0.40 eV per H<sub>2</sub> with a gravimetric density of 5.5 wt% are deemed appropriate for hydrogen storage. The 2D materials are among the leading materials for hydrogen storage, as they satisfy all prerequisites. To this end, borophene is expected to exhibit even higher performance than that of graphene. Er et al.<sup>[33]</sup> have predicted an improved hydrogen storage capacity of a planar borophene sheet (0.15 eV per H<sub>2</sub>) by DFT first-principle calculations using VASP. Through DFT calculations, it has been predicted that Ca- and Li-doped borophene structures exhibit excellent hydrogen storage capabilities (0.142 and 0.176 eV per H<sub>2</sub>) in comparison to that of planar borophene sheets, respectively. Li et al. and Wang et al. have improved these storage capacities by introducing Ca atoms onto borophene sheets to values of 0.20–0.32 eV per H<sub>2</sub>, obtained by first-principle calculations using VASP.<sup>[35]</sup> The protrusions, ridges, edges, and defects in borophene sheets could act as anchoring sites for hydrogen atoms. Moreover, the ability of boron to form borane gas (BH<sub>3</sub>) upon reaction with hydrogen makes the borophene sheets (larger surface area than that of bulk boron) more prone to react with hydrogen gas.

## 5.3. Superconductors

Among the 2D materials, Dirac materials are being extensively investigated owing to the superconducting behaviors attributed to their strong electron–phonon couplings. Graphene sheets with monolayer, bilayer (1.1° twist,  $T_c \approx 2$  K),<sup>[36]</sup> and trilayer thicknesses have been investigated. Extensive studies are required to demonstrate its superconducting properties. Results have suggested that graphene doped with heavier atoms is superconducting.<sup>[37]</sup> Borophene, another Dirac material, has not been extensively studied in terms of superconductivity. Penev et al.<sup>[23]</sup> have analyzed the electronic structures, phonon spectra, and electron–phonon couplings of 2D boron polymorphs and reported that a 2D sheet of borophene exhibits intrinsic phonon-mediated superconductivity ( $T_c \approx 10$ –20 K). Free-standing borophene sheets are also considered the best-suited materials for alkali battery, electric, and heterocatalytic applications. However, applications of free-standing borophene

sheets in these promising fields have not been reported. Therefore, it is too early to discuss its further applications in the field of energy generation.

## 5.4. Energy Storage

Graphene is charge-neutral without electrons in its  $p_z$  orbital. All electrons are utilized in the  $sp^2$  hybridization, making graphene chemistry-passive. Therefore, mostly, it does not react under ambient conditions. For electrochemical oxidation/reduction reactions, active sites, and low adsorption energy are desirable, which can facilitate the redox reaction. The specific capacitance of free-standing borophene oxide has been investigated by Ranjan et al.<sup>[29a]</sup> It has exhibited a superior value to those of other 2D materials. However, doped graphene has been considered the best-suited material for such applications. In contrast, borophene is metallic with abundant electrons, particularly along ridgelines. Moreover, sufficient spaces exist between the ridgelines, which can act as channels for ion movement along the ridge direction. Zhang et al.<sup>[38]</sup> and Mortazavi et al.<sup>[39]</sup> have theoretically demonstrated the higher specific capacities of the  $\beta_{12}$  and X<sub>3</sub> phases of borophene for Li- and Na-electrode materials than those of other reported 2D materials. The predicted specific capacity of the X<sub>3</sub> phase is 1240 mAh g<sup>−1</sup>, while that of the  $\beta_{12}$  phase is more than 1.5 times (1984 mAh g<sup>−1</sup>) that of the X<sub>3</sub> phase owing to the structural anisotropy. Jiang et al.<sup>[30a]</sup> and Shi et al.<sup>[40]</sup> have calculated (DFT) the adsorption energies of the  $\beta_{12}$  and X<sub>3</sub> phases and predicted that the migration energies of the  $\beta_{12}$  and X<sub>3</sub> phases of borophene in a Na-ion battery are almost half of those in a Li-ion battery. Therefore, the  $\beta_{12}$  and X<sub>3</sub> phases of borophene are more suited for Na-ion batteries than for Li-ion batteries.

## 6. Summary and Perspective

Within a short period of time, it has been demonstrated that 2D materials have high application potentials (Figure 11).<sup>[2c,42]</sup> Borophene gradually becomes a favorite material owing to its unique electronic properties suitable for various applications. Various strategies have been used for the synthesis of borophene, including ALD, CVD, MBE, and sonochemical exfoliation. The combined approach of chemical exfoliation and sonochemical exfoliation has been used for the bulk synthesis of borophene nanosheets. We surmise that most of the synthesis techniques for graphene<sup>[41]</sup> may also be used for the synthesis of borophene with different phases. The synthesis techniques including crystal growth techniques such as deposition of borophene sheets by pulsed laser deposition, laser chemical vapor deposition (physical vapor route), microwave-assisted approach, intercalation-based exfoliation, and laser-based exfoliation, which have been successfully used for the synthesis of graphene, may be investigated for the synthesis of borophene in the near future.

Borophene is metallic even at one layer and perhaps the lightest 2D material. The substrate-supported borophene has limitations, while free-standing sheets are unique with promising electronic properties for novel applications.



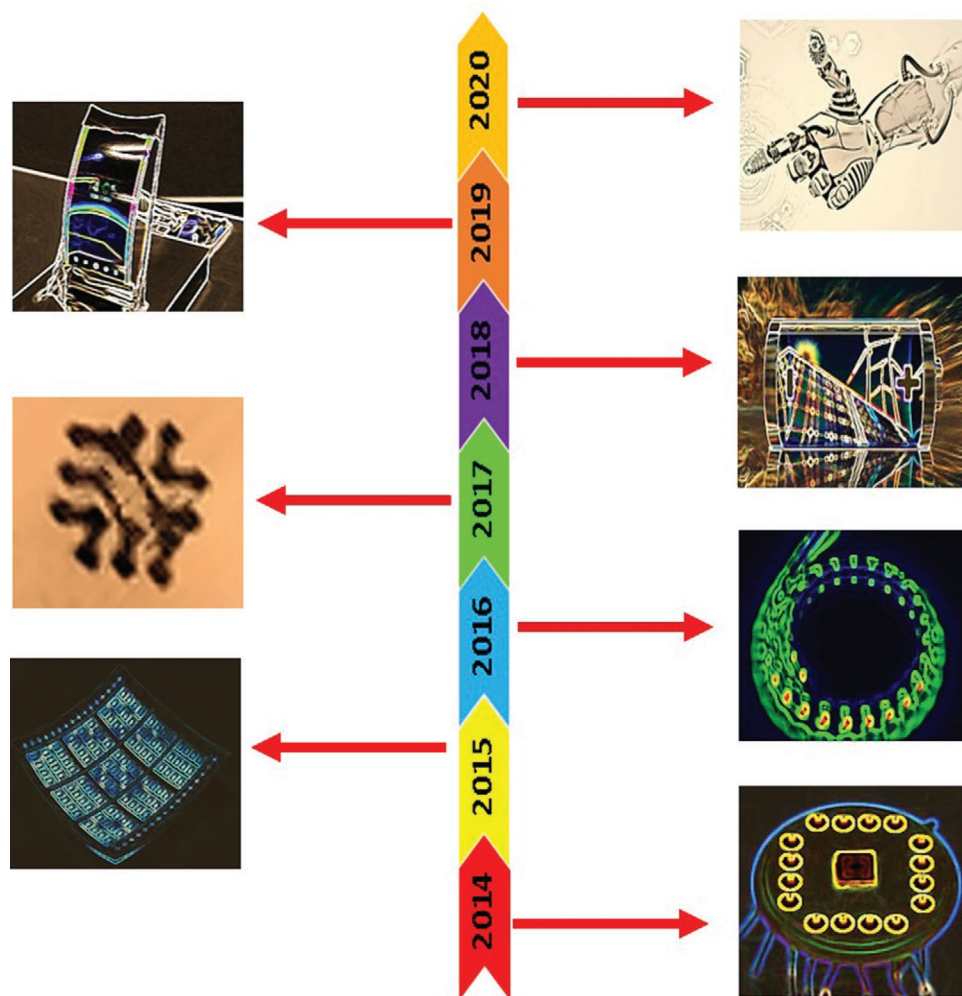


**Figure 11.** Futuristic technological applications of 2D material.

Real devices and sensors have become available in nearby shops. Borophene may be used in numerous frontline applications, including flexible electronic chips, fire alarms, prompt gas sensors, field-effect transistors, anticorrosion, deoxyribonucleic acid sensing, and solar cells (**Figure 12**). Automated household switching based on photosensing hybrids such as borophene–molybdenum disulfide, borophene–phosphorene, and borophene–graphene oxide is another potential application.

Even though borophene is the most recent superior 2D material with a high potential, numerous challenges need to be overcome for its applications (**Figure 13**).<sup>[43]</sup> The practical realization of free-standing borophene has been deemed challenging owing to the existing theories that it cannot crystallize without substrate and as the 3D boron crystal is not a van der Waals material. Similar to graphene, borophene can be strain-engineered to open a bandgap.<sup>[43]</sup> For example, graphene nanoribbons have been synthesized and employed for various sensing applications. The sensitivity is usually increased when graphene is in the nanoribbon form owing to the edge states.<sup>[41e,j]</sup> It is expected that borophene may exhibit higher performances than those of graphene owing to its unique electronic properties. In

the future, the energy demand would be high and green energy would be preferred. Thus, hydrogen-based energy would be suitable. In this regard, a considerably better reversible energy storage by the  $\beta_{12}$  phase of borophene is expected.<sup>[44]</sup> As graphene has been employed as an excellent shield for ultraviolet lasers, borophene, metallic with abundant electrons, may also be useful for such applications.<sup>[45]</sup> Graphene with the excellent thermal conduction promptly removes unwanted heat from interfaces and is suitable for a SERS-based molecular sensing where a high-intensity laser is used and the interfacial heating, particularly at the plasmonic tip, degrades the molecules to be diagnosed.<sup>[46]</sup> The application of borophene in SERS has been envisioned by Ranjan et al.<sup>[29a]</sup> We expect numerous SERS-based sensing devices with borophene in the near future.

Borophene could be used in terahertz guiding applications. The abundant electrons in the metallic borophene crystal can act as an excellent anchor for various chemical reactions and thus it can be employed for catalysis. Heterolayered devices based on hybridizations with carbon or nitride nanostructures will pave the way for new applications. For example, sensors consisting of borophene and other 2D materials can be promising future devices considering the realization of electronic,

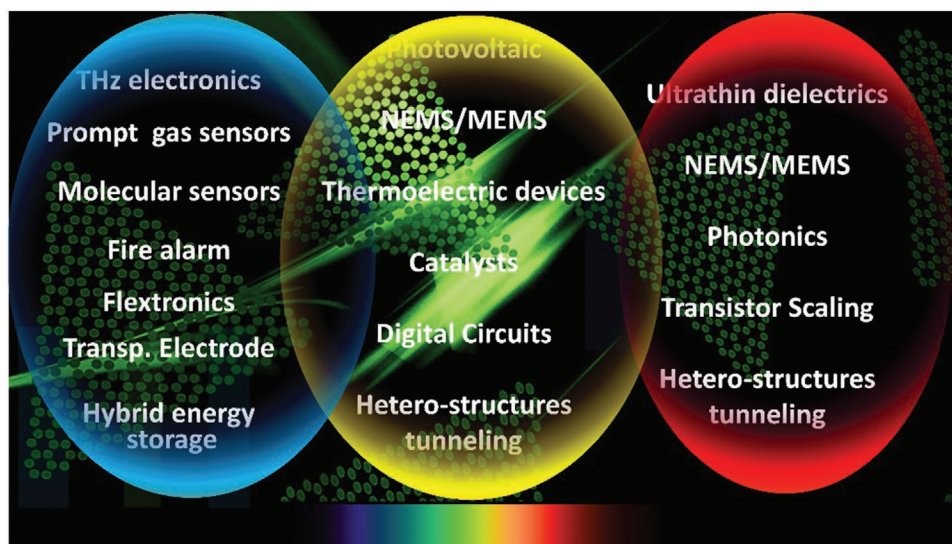


**Figure 12.** Schematic representation showing various applications of 2D materials in different spectroscopic ranges.

photonic, and thermal metamaterials. The increased electronic mobility of graphene in the vicinity of BN is of interest. We expect that borophene behaves similarly. Quantum mechanical sensors and magnetic tunnel devices are being proposed. However, the fabrication of such devices is quite challenging. Recently, Kumar et al.<sup>[47]</sup> have demonstrated a graphene/BN/graphene heterolayer as an excellent candidate for electronic tunneling as well as an anchor for single-photon emitters.

A similar strategy may be applicable to borophene and phosphorene (new family members), which can act as essential building blocks for the future fabrication of heterolayer devices and sensors.

Briefly, borophene has progressed from conception to realization and is extensively studied for practical applications. It could be employed as a replacement for graphene in several applications (terahertz applications, strengthening of plastics<sup>[13h,48]</sup>). In

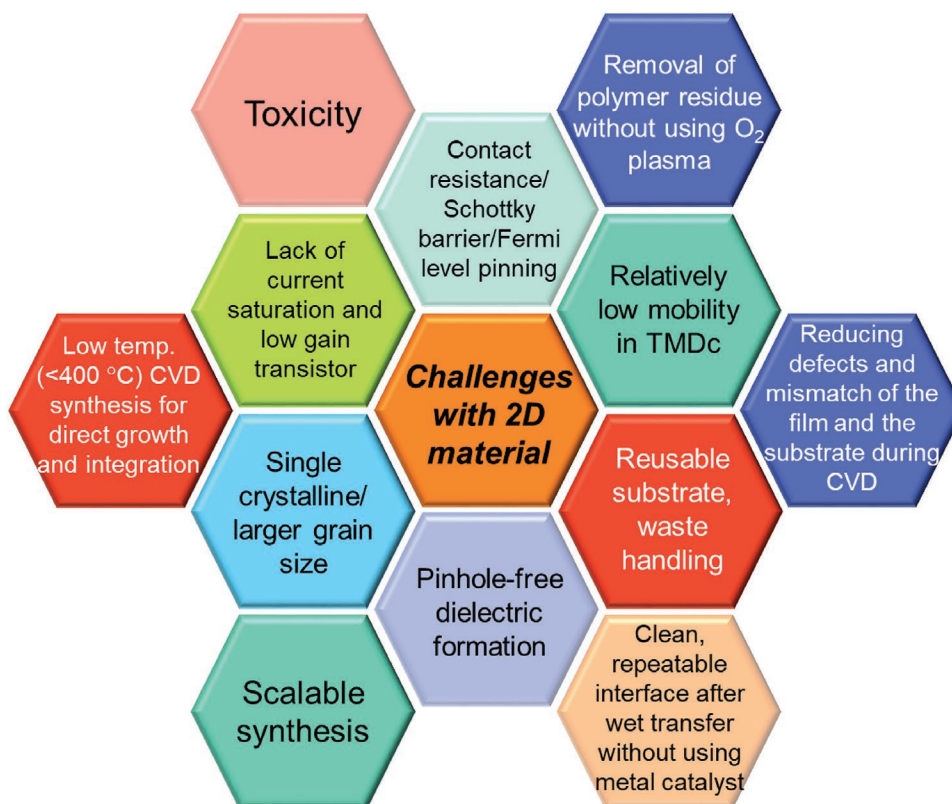


**Figure 13.** Challenges faced by 2D materials from synthesis to device applications.

addition, we strongly believe that borophene will exhibit even higher performances owing to the increased electronic density along ridgelines and improved elastic behavior along the ridge. As graphene has pushed the boundaries of science and engineering and changed the industries, borophene, lighter with abundant electrons, compared to graphene, would be a new cutting-edge material in the near future. The progress on borophene has been outstanding, but its high potentials are yet to be utilized. Borophene is a unique material with intriguing bonding capabilities and unprecedented physical and chemical behaviors for various instant and long-term applications. The existing scientific literature, including review articles and book chapters, presents the specific characteristics of borophene, but without focusing on broad commercial applications facilitating the human life. This comprehensive review could largely advance the emerging technologies based on borophene.

## Acknowledgements

The authors acknowledge the Department of Science and Technology, Govt. of India, for the Research grant under Ramanujan Fellowship (Sanction No. SB/S2/RJN-205/2014). A.V. thanks the Australian Research Council (DP 170104478 and DP 150104828) and the University of Newcastle for the funding.

## Conflict of Interest

The authors declare no conflict of interest.

## Keywords

2D materials, borophene, free-standing borophene, solution-phase exfoliation, substrate-supported growth

Received: January 22, 2020

Revised: April 29, 2020

Published online: July 14, 2020

- [1] a) A. K. Geim, K. S. Novoselov, *Nat. Mater.* **2007**, *6*, 183; b) A. H. Castro Neto, F. Guinea, N. M. R. Peres, K. S. Novoselov, A. K. Geim, *Rev. Mod. Phys.* **2009**, *81*, 109; c) Y. Saito, T. Nojima, Y. Iwasa, *Nat. Rev. Mater.* **2017**, *2*, 16094.
- [2] a) C. Huo, Z. Yan, X. Song, H. Zeng, *Sci. Bull.* **2015**, *60*, 1994; b) W.-G. Kim, S. Nair, *Chem. Eng. Sci.* **2013**, *104*, 908; c) X. Zhang, L. Hou, A. Ciesielski, P. Samori, *Adv. Energy Mater.* **2016**, *6*, 1600671.
- [3] a) G. Choi, S. Eom, A. Vinu, J.-H. Choy, *Chem. Rec.* **2018**, *18*, 1033; b) G. Singh, I. S. Ismail, C. Bilen, D. Shanbhag, C. I. Sathish, K. Ramadass, A. Vinu, *Appl. Energy* **2019**, *255*, 113831.
- [4] a) M. Macha, S. Marion, V. V. R. Nandigana, A. Radenovic, *Nat. Rev. Mater.* **2019**, *4*, 588; b) X. Liu, M. C. Hersam, *Nat. Rev. Mater.* **2019**, *4*, 669; c) B. Feng, Z. Ding, S. Meng, Y. Yao, X. He, P. Cheng, L. Chen, K. Wu, *Nano Lett.* **2012**, *12*, 3507; d) Y. Du, J. Zhuang, H. Liu, X. Xu, S. Eilers, K. Wu, P. Cheng, J. Zhao, X. Pi, K. W. See, G. Peleckis, X. Wang, S. X. Dou, *ACS Nano* **2014**, *8*, 10019; e) L. Li, S.-Z. Lu, J. Pan, Z. Qin, Y.-Q. Wang, Y. Wang, G. Cao, S. Du, H.-J. Gao, *Adv. Mater.* **2014**, *26*, 4820; f) Z. Li, J. Zhuang, L. Chen, Z. Ni, C. Liu, L. Wang, X. Xu, J. Wang, X. Pi, X. Wang, Y. Du, K. Wu, S. X. Dou, *ACS Cent. Sci.* **2016**, *2*, 517; g) Y. Du, J. Zhuang, J. Wang, Z. Li, H. Liu, J. Zhao, X. Xu, H. Feng, L. Chen, K. Wu, X. Wang, S. X. Dou, *Sci. Adv.* **2016**, *2*, e1600067; h) Y. Xu, B. Yan, H.-J. Zhang, J. Wang, G. Xu, P. Tang, W. Duan, S.-C. Zhang, *Phys. Rev. Lett.* **2013**, *111*, 136804; i) J. Zhuang, X. Xu, G. Peleckis, W. Hao, S. X. Dou, Y. Du, *Adv. Mater.* **2017**, *29*, 1606716; j) J. Zhuang, N. Gao, Z. Li, X. Xu, J. Wang, J. Zhao, S. X. Dou, Y. Du, *ACS Nano* **2017**, *11*, 3553; k) J. Zhuang, C. Liu, Z. Zhou, G. Casillas, H. Feng, X. Xu, J. Wang, W. Hao, X. Wang, S. X. Dou, Z. Hu, Y. Du, *Adv. Sci.* **2018**, *5*, 1800207; l) J. L. Zhang, S. Zhao, C. Han, Z. Wang, S. Zhong, S. Sun, R. Guo, X. Zhou, C. D. Gu, K. D. Yuan, Z. Li, W. Chen, *Nano Lett.* **2016**, *16*, 4903; m) J. Zhuang, C. Liu, Q. Gao, Y. Liu, H. Feng, X. Xu, J. Wang, J. Zhao, S. X. Dou, Z. Hu, Y. Du, *ACS Nano* **2018**, *12*, 5059; n) Z. Li, J. Zhuang, L. Wang, H. Feng, Q. Gao, X. Xu, W. Hao, X. Wang, C. Zhang, K. Wu, S. X. Dou, L. Chen, Z. Hu, Y. Du, *Sci. Adv.* **2018**, *4*, eaau4511; o) S. K. Apte, S. N. Garaje, G. P. Mane, A. Vinu, S. D. Naik, D. P. Amalnerkar, B. B. Kale, *Small* **2011**, *7*, 957; p) Q. Ji, I. Honma, S. M. Paek, M. Akada, J. P. Hill, A. Vinu, K. Ariga, *Angew. Chem., Int. Ed.* **2010**, *49*, 9737; q) D. P. Dubal, N. R. Chodankar, A. Vinu, D. H. Kim, P. Gomez-Romero, *ChemSusChem* **2017**, *10*, 2742; r) I. Y. Kim, S. Kim, X. Jin, S. Premkumar, G. Chandra, N. S. Lee, G. P. Mane, S.-J. Hwang, S. Umapathy, A. Vinu, *Angew. Chem., Int. Ed.* **2018**, *130*, 17281; s) K. S. Lakhi, D. H. Park, K. Al-Bahily, W. Cha, B. Viswanathan, J. H. Choy, A. Vinu, *Chem. Soc. Rev.* **2017**, *46*, 72; t) S. N. Talapaneni, G. Singh, I. Y. Kim, K. Al-Bahily, A. H. Al-Muhtaseb, A. S. Karakoti, E. Tavakkoli, A. Vinu, *Adv. Mater.* **2020**, *32*, 1904635.
- [5] a) Z.-Q. Wang, T.-Y. Lü, H.-Q. Wang, Y. P. Feng, J.-C. Zheng, *Front. Phys.* **2019**, *14*, 33403; b) J. Tian, Z. Xu, C. Shen, F. Liu, N. Xu, H.-J. Gao, *Nanoscale* **2010**, *2*, 1375; c) A. J. Mannix, Z. Zhang, N. P. Guisinger, B. I. Yakobson, M. C. Hersam, *Nat. Nanotechnol.* **2018**, *13*, 444; d) D. Ayodhya, G. Veerabhadram, *FlatChem* **2020**, *19*, 100150; e) D. Li, J. Gao, P. Cheng, J. He, Y. Yin, Y. Hu, L. Chen, Y. Cheng, J. Zhao, *Adv. Funct. Mater.* **2020**, *30*, 1904349; f) S.-Y. Xie, Y. Wang, X.-B. Li, *Adv. Mater.* **2019**, *31*, 1900392.
- [6] a) W. Li, L. Kong, C. Chen, J. Gou, S. Sheng, W. Zhang, H. Li, L. Chen, P. Cheng, K. Wu, *Sci. Bull.* **2018**, *63*, 282; b) L. Z. Zhang, Q. B. Yan, S. X. Du, G. Su, H. J. Gao, *J. Phys. Chem. C* **2012**, *116*, 18202; c) B. Kiraly, X. Liu, L. Wang, Z. Zhang, A. J. Mannix, B. L. Fisher, B. I. Yakobson, M. C. Hersam, N. P. Guisinger, *ACS Nano* **2019**, *13*, 3816; d) R. Wu, I. K. Drozdov, S. Eltinge, P. Zahl, S. Ismail-Beigi, I. Božović, A. Gozar, *Nat. Nanotechnol.* **2019**, *14*, 44; e) Y. Tian, Z. Guo, T. Zhang, H. Lin, Z. Li, J. Chen, S. Deng, F. Liu, *Nanomaterials* **2019**, *9*, 538; f) G. Tai, T. Hu, Y. Zhou, X. Wang, J. Kong, T. Zeng, Y. You, Q. Wang, *Angew. Chem., Int. Ed.* **2015**, *54*, 15473; g) D. Li, Y. Chen, J. He, Q. Tang, C. Zhong, G. Ding, *Chin. Phys. B* **2018**, *27*, 036303; h) X. Liu, L. Wang, S. Li, M. S. Rahn, B. I. Yakobson, M. C. Hersam, *Nat. Commun.* **2019**, *10*, 1642.
- [7] a) M. Fujimori, T. Nakata, T. Nakayama, E. Nishibori, K. Kimura, M. Takata, M. Sakata, *Phys. Rev. Lett.* **1999**, *82*, 4452; b) X. Sun, X. Liu, J. Yin, J. Yu, Y. Li, Y. Hang, X. Zhou, M. Yu, J. Li, G. Tai, W. Guo, *Adv. Funct. Mater.* **2017**, *27*, 1603300.
- [8] a) T. Jian, X. Chen, S.-D. Li, A. I. Boldyrev, J. Li, L.-S. Wang, *Chem. Soc. Rev.* **2019**, *48*, 3550; b) Research by Prof. Lai-Sheng Wang's group at Brown University, [http://casey.brown.edu/chemistry/research/LSWang/research/fullscreen\\_research.html](http://casey.brown.edu/chemistry/research/LSWang/research/fullscreen_research.html) (accessed: June 2020).
- [9] a) K. S. Novoselov, A. K. Geim, S. V. Morozov, D. Jiang, Y. Zhang, S. V. Dubonos, I. V. Grigorieva, A. A. Firsov, *Science* **2004**, *306*, 666; b) H. Liu, A. T. Neal, Z. Zhu, Z. Luo, X. Xu, D. Tománek, P. D. Ye, *ACS Nano* **2014**, *8*, 4033; c) H. Tang, S. Ismail-Beigi, *Phys. Rev. Lett.* **2007**, *99*, 115501; d) X. Yang, Y. Ding, J. Ni, *Phys. Rev. B* **2008**, *77*, 41402.
- [10] K. I. Bolotin, K. J. Sikes, Z. Jiang, M. Klima, G. Fudenberg, J. Hone, P. Kim, H. L. Stormer, *Solid State Commun.* **2008**, *146*, 351.
- [11] F. Schwierz, J. Pezoldt, R. Granzner, *Nanoscale* **2015**, *7*, 8261.



- [12] L. Li, Y. Yu, G. J. Ye, Q. Ge, X. Ou, H. Wu, D. Feng, X. H. Chen, Y. Zhang, *Nat. Nanotechnol.* **2014**, 9, 372.
- [13] a) R. Fivaz, E. Mooser, *Phys. Rev.* **1967**, 163, 743; b) B. Radisavljevic, A. Radenovic, J. Brivio, V. Giacometti, A. Kis, *Nat. Nanotechnol.* **2011**, 6, 147; c) F. Withers, T. H. Bointon, D. C. Hudson, M. F. Craciun, S. Russo, *Sci. Rep.* **2015**, 4, 4967; d) D. Braga, I. Gutiérrez Lezama, H. Berger, A. F. Morpurgo, *Nano Lett.* **2012**, 12, 5218; e) H. Y. Lv, W. J. Lu, D. F. Shao, Y. Liu, S. G. Tan, Y. P. Sun, *EPL* **2015**, 110, 37004; f) X. Wang, Y. Gong, G. Shi, W. L. Chow, K. Keyshar, G. Ye, R. Vajtai, J. Lou, Z. Liu, E. Ringe, B. K. Tay, P. M. Ajayan, *ACS Nano* **2014**, 8, 5125; g) D. H. Keum, S. Cho, J. H. Kim, D.-H. Choe, H.-J. Sung, M. Kan, H. Kang, J.-Y. Hwang, S. W. Kim, H. Yang, K. J. Chang, Y. H. Lee, *Nat. Phys.* **2015**, 11, 482; h) L. Wang, I. Meric, P. Y. Huang, Q. Gao, Y. Gao, H. Tran, T. Taniguchi, K. Watanabe, L. M. Campos, D. A. Muller, J. Guo, P. Kim, J. Hone, K. L. Shepard, C. R. Dean, *Science* **2013**, 342, 614; i) A. Allain, A. Kis, *ACS Nano* **2014**, 8, 7180; j) D. E. Soule, *Phys. Rev.* **1958**, 112, 698.
- [14] T. Cheng, H. Lang, Z. Li, Z. Liu, Z. Liu, *Phys. Chem. Chem. Phys.* **2017**, 19, 23942.
- [15] A. J. Mannix, X.-F. Zhou, B. Kiraly, J. D. Wood, D. Alducin, B. D. Myers, X. Liu, B. L. Fisher, U. Santiago, J. R. Guest, M. J. Yacamán, A. Ponce, A. R. Oganov, M. C. Hersam, N. P. Guisinger, *Science* **2015**, 350, 1513.
- [16] a) A. Cepellotti, G. Fugallo, L. Paulatto, M. Lazzeri, F. Mauri, N. Marzari, *Nat. Commun.* **2015**, 6, 6400; b) G. Qin, Z. Qin, W.-Z. Fang, L.-C. Zhang, S.-Y. Yue, Q.-B. Yan, M. Hu, G. Su, *Nanoscale* **2016**, 8, 11306; c) X. Gu, R. Yang, *Appl. Phys. Lett.* **2014**, 105, 131903; d) X. Wu, V. Varshney, J. Lee, Y. Pang, A. K. Roy, T. Luo, *Chem. Phys. Lett.* **2017**, 669, 233; e) T. Liang, P. Zhang, P. Yuan, S. Zhai, D. Yang, *Nano Futures* **2019**, 3, 015001; f) J. Zhang, H. J. Liu, L. Cheng, J. Wei, J. H. Liang, D. D. Fan, P. H. Jiang, J. Shi, *Sci. Rep.* **2017**, 7, 4623; g) R. Yan, J. R. Simpson, S. Bertolazzi, J. Brivio, M. Watson, X. Wu, A. Kis, T. Luo, A. R. Hight Walker, H. G. Xing, *ACS Nano* **2014**, 8, 986; h) D. Li, J. He, G. Ding, Q. Tang, Y. Ying, J. He, C. Zhong, Y. Liu, C. Feng, Q. Sun, H. Zhou, P. Zhou, G. Zhang, *Adv. Funct. Mater.* **2018**, 28, 1801685; i) B. Mortazavi, M. Makaremi, M. Shahrokhi, M. Raeisi, C. V. Singh, T. Rabczuk, L. F. C. Pereira, *Nanoscale* **2018**, 10, 3759; j) H. Zhou, Y. Cai, G. Zhang, Y.-W. Zhang, *npj 2D Mater. Appl.* **2017**, 1, 14; k) G. Liu, H. Wang, Y. Gao, J. Zhou, H. Wang, *Phys. Chem. Chem. Phys.* **2017**, 19, 2843; l) H. Sun, Q. Li, X. G. Wan, *Phys. Chem. Chem. Phys.* **2016**, 18, 14927; m) M. Q. L. B. Mortazavi, T. Rabczuk, L. F. C. Pereira, *Phys. E* **2017**, 93, 202; n) H. Xiao, W. Cao, T. Ouyang, S. Guo, C. He, J. Zhong, *Sci. Rep.* **2017**, 7, 45986; o) X. Gu, R. Yang, *J. Appl. Phys.* **2015**, 117, 025102; p) G. Qin, Q.-B. Yan, Z. Qin, S.-Y. Yue, M. Hu, G. Su, *Phys. Chem. Chem. Phys.* **2015**, 17, 4854.
- [17] a) C. Zhong, Y. Chen, Z.-M. Yu, Y. Xie, H. Wang, S. A. Yang, S. Zhang, *Nat. Commun.* **2017**, 8, 15641; b) C. Zhong, Y. Chen, Y. Xie, S. A. Yang, M. L. Cohen, S. B. Zhang, *Nanoscale* **2016**, 8, 7232.
- [18] F. Ma, Y. Jiao, G. Gao, Y. Gu, A. Bilic, Z. Chen, A. Du, *Nano Lett.* **2016**, 16, 3022.
- [19] H. Zhang, Y. Xie, Z. Zhang, C. Zhong, Y. Li, Z. Chen, Y. Chen, *J. Phys. Chem. Lett.* **2017**, 8, 1707.
- [20] B. Feng, O. Sugino, R.-Y. Liu, J. Zhang, R. Yukawa, M. Kawamura, T. Iimori, H. Kim, Y. Hasegawa, H. Li, L. Chen, K. Wu, H. Kumigashira, F. Komori, T.-C. Chiang, S. Meng, I. Matsuda, *Phys. Rev. Lett.* **2017**, 118, 096401.
- [21] a) B. Mortazavi, O. Rahaman, A. Dianat, T. Rabczuk, *Phys. Chem. Chem. Phys.* **2016**, 18, 27405; b) Q. Wei, X. Peng, *Appl. Phys. Lett.* **2014**, 104, 251915; c) Z. Wang, T.-Y. Lü, H.-Q. Wang, Y. P. Feng, J.-C. Zheng, *Phys. Chem. Chem. Phys.* **2016**, 18, 31424; d) M. Q. Le, B. Mortazavi, T. Rabczuk, *Nanotechnology* **2016**, 27, 445709; e) Y.-P. Zhou, J.-W. Jiang, *Sci. Rep.* **2017**, 7, 45516; f) W.-C. Yi, W. Liu, J. Botana, L. Zhao, Z. Liu, J.-Y. Liu, M.-S. Miao, *J. Phys. Chem. Lett.* **2017**, 8, 2647.
- [22] a) R. C. Andrew, R. E. Mapasha, A. M. Ukpong, N. Chetty, *Phys. Rev. B* **2012**, 85, 125428; b) Z.-Q. Wang, H. Cheng, T.-Y. Lü, H.-Q. Wang, Y. P. Feng, J.-C. Zheng, *Phys. Chem. Chem. Phys.* **2018**, 20, 16510; c) T. Li, *Phys. Rev. B* **2012**, 85, 235407.
- [23] E. S. Penev, S. Bhowmick, A. Sadrzadeh, B. I. Yakobson, *Nano Lett.* **2012**, 12, 2441.
- [24] a) X. Wu, J. Dai, Y. Zhao, Z. Zhuo, J. Yang, X. C. Zeng, *ACS Nano* **2012**, 6, 7443; b) Z. Zhang, Y. Yang, E. S. Penev, B. I. Yakobson, *Adv. Funct. Mater.* **2017**, 27, 1605059.
- [25] B. Feng, J. Zhang, Q. Zhong, W. Li, S. Li, H. Li, P. Cheng, S. Meng, L. Chen, K. Wu, *Nat. Chem.* **2016**, 8, 563.
- [26] R. Wu, A. Gozar, I. Božović, *npj Quantum Mater.* **2019**, 4, 40.
- [27] a) N. Karmodak, E. D. Jemmis, *Angew. Chem., Int. Ed.* **2017**, 56, 10093; b) N. Karmodak, E. D. Jemmis, *J. Phys. Chem. C* **2018**, 122, 2268.
- [28] J. N. Coleman, *Acc. Chem. Res.* **2013**, 46, 14.
- [29] a) P. Ranjan, T. K. Sahu, R. Bhushan, S. S. Yamijala, D. J. Late, P. Kumar, A. Vinu, *Adv. Mater.* **2019**, 31, 1900353; b) H. Li, L. Jing, W. Liu, J. Lin, R. Y. Tay, S. H. Tsang, E. H. T. Teo, *ACS Nano* **2018**, 12, 1262; c) X. Ji, N. Kong, J. Wang, W. Li, Y. Xiao, S. T. Gan, Y. Zhang, Y. Li, X. Song, Q. Xiong, S. Shi, Z. Li, W. Tao, H. Zhang, L. Mei, J. Shi, *Adv. Mater.* **2018**, 30, 1803031.
- [30] a) H. R. Jiang, Z. Lu, M. C. Wu, F. Ciucci, T. S. Zhao, *Nano Energy* **2016**, 23, 97; b) Q. H. Wang, K. Kalantar-Zadeh, A. Kis, J. N. Coleman, M. S. Strano, *Nat. Nanotechnol.* **2012**, 7, 699.
- [31] R. R. Nair, P. Blake, A. N. Grigorenko, K. S. Novoselov, T. J. Booth, T. Stauber, N. M. R. Peres, A. K. Geim, *Science* **2008**, 320, 1308.
- [32] D. O. Lindroth, P. Erhart, *Phys. Rev. B* **2016**, 94, 115205.
- [33] a) S. H. Mir, S. Chakraborty, P. C. Jha, J. Wörn, H. Soni, P. K. Jha, R. Ahuja, *Appl. Phys. Lett.* **2016**, 109, 053903; b) Y. Chen, G. Yu, W. Chen, Y. Liu, G.-D. Li, P. Zhu, Q. Tao, Q. Li, J. Liu, X. Shen, H. Li, X. Huang, D. Wang, T. Asefa, X. Zou, *J. Am. Chem. Soc.* **2017**, 139, 12370; c) Y. Singh, S. Back, Y. Jung, *Phys. Chem. Chem. Phys.* **2018**, 20, 21095; d) Y. Wang, J. Fan, M. Trenary, *Chem. Mater.* **1993**, 5, 192; e) S. Er, G. A. de Wijs, G. Brocks, *J. Phys. Chem. C* **2009**, 113, 18962.
- [34] a) H. Cui, X. Zhang, D. Chen, *Appl. Phys. A* **2018**, 124, 636; b) C.-S. Huang, A. Murat, V. Babar, E. Montes, U. Schwingenschlög, *J. Phys. Chem. C* **2018**, 122, 14665; c) T. Liu, Y. Chen, M. Zhang, L. Yuan, C. Zhang, J. Wang, J. Fan, *AIP Adv.* **2017**, 7, 125007; d) A. Omidvar, *Comput. Theor. Chem.* **2017**, 1115, 179; e) V. Shukla, J. Wörn, N. K. Jena, A. Grigoriev, R. Ahuja, *J. Phys. Chem. C* **2017**, 121, 26869.
- [35] a) J. Wang, Y. Du, L. Sun, *Int. J. Hydrogen Energy* **2016**, 41, 5276; b) L. Li, H. Zhang, X. Cheng, *Comput. Mater. Sci.* **2017**, 137, 119.
- [36] Y. Cao, V. Fatemi, S. Fang, K. Watanabe, T. Taniguchi, E. Kaxiras, P. Jarillo-Herrero, *Nature* **2018**, 556, 43.
- [37] J. Chapman, Y. Su, C. A. Howard, D. Kundys, A. N. Grigorenko, F. Guinea, A. K. Geim, I. V. Grigorieva, R. R. Nair, *Sci. Rep.* **2016**, 6, 23254.
- [38] X. Zhang, J. Hu, Y. Cheng, H. Y. Yang, Y. Yao, S. A. Yang, *Nanoscale* **2016**, 8, 15340.
- [39] B. Mortazavi, A. Dianat, O. Rahaman, G. Cuniberti, T. Rabczuk, *J. Power Sources* **2016**, 329, 456.
- [40] L. Shi, T. Zhao, A. Xu, J. Xu, *Sci. Bull.* **2016**, 61, 1138.
- [41] a) P. Kumar, *RSC Adv.* **2013**, 3, 11987; b) Y. Hernandez, V. Nicolosi, M. Lotya, F. M. Blighe, Z. Sun, S. De, I. T. McGovern, B. Holland, M. Byrne, Y. K. Gun'ko, J. J. Boland, P. Niraj, G. Duesberg, S. Krishnamurthy, R. Goodhue, J. Hutchison, V. Scardaci, A. C. Ferrari, J. N. Coleman, *Nat. Nanotechnol.* **2008**, 3, 563; c) S. Bae, H. Kim, Y. Lee, X. Xu, J.-S. Park, Y. Zheng, J. Balakrishnan, T. Lei, H. Ri Kim, Y. I. Song, Y.-J. Kim, K. S. Kim, B. Özyilmaz, J.-H. Ahn, B. H. Hong, S. Iijima, *Nat. Nanotechnol.* **2010**, 5, 574; d) D. Voiry, J. Yang, J. Kuperberg, R. Fullon, C. Lee, H. Y. Jeong, H. S. Shin, M. Chhowalla, *Science* **2016**, 353, 1413; e) P. Kumar, L. S. Panchakarla, C. N. R. Rao, *Nanoscale* **2011**, 3, 2127; f) K. S. S. P. Kumar, C. N. R. Rao, *Int. J. Nanosci.* **2011**, 10, 559;

- g) P. Ranjan, P. Tiwary, A. K. Chakraborty, R. Mahapatra, A. D. Thakur, *J. Mater. Sci.: Mater. Electron.* **2018**, 29, 15946; h) C. N. R. Rao, K. S. Subrahmanyam, H. S. S. Ramakrishna Matte, B. Abdulhakeem, A. Govindaraj, B. Das, P. Kumar, A. Ghosh, D. J. Late, *Sci. Technol. Adv. Mater.* **2010**, 11, 054502; i) U. Maitra, H. S. S. R. Matte, P. Kumar, C. N. R. Rao, *Chimia* **2012**, 66, 941; j) P. Kumar, S. S. R. K. C. Yamijala, S. K. Pati, *J. Phys. Chem. C* **2016**, 120, 16985; k) K. Vasu, S. S. R. K. C. Yamijala, A. Zak, K. Gopalakrishnan, S. K. Pati, C. N. R. Rao, *Small* **2015**, 11, 3916; l) H. S. S. R. Matte, U. Maitra, P. Kumar, B. Govinda Rao, K. Pramoda, C. N. R. Rao, *Z. Anorg. Allg. Chem.* **2012**, 638, 2617.
- [42] a) R. Mas-Ballesté, C. Gómez-Navarro, J. Gómez-Herrero, F. Zamora, *Nanoscale* **2011**, 3, 20; b) Z. Lin, A. McCreary, N. Briggs, S. Subramanian, K. Zhang, Y. Sun, X. Li, N. J. Borys, H. Yuan, S. K. Fullerton-Shirey, A. Chernikov, H. Zhao, S. McDonnell, A. M. Lindenberg, K. Xiao, B. J. LeRoy, M. Drndić, J. C. M. Hwang, J. Park, M. Chhowalla, R. E. Schaak, A. Javey, M. C. Hersam, J. Robinson, M. Terrones, *2D Mater.* **2016**, 3, 042001; c) P. Ranjan, S. Agrawal, A. Sinha, T. R. Rao, J. Balakrishnan, A. D. Thakur, *Sci. Rep.* **2018**, 8, 12007; d) P. Ranjan, Tulika, R. Laha, J. Balakrishnan, *J. Raman Spectrosc.* **2017**, 48, 586; e) J. Liu, L. Fu, *Adv. Mater.* **2019**, 31, 1800690.
- [43] M. Motlag, P. Kumar, K. Y. Hu, S. Jin, J. Li, J. Shao, X. Yi, Y.-H. Lin, J. C. Walrath, L. Tong, X. Huang, R. S. Goldman, L. Ye, G. J. Cheng, *Adv. Mater.* **2019**, 31, 1900597.
- [44] K. S. Subrahmanyam, P. Kumar, U. Maitra, A. Govindaraj, K. P. S. S. Hembram, U. V. Waghmare, C. N. R. Rao, *Proc. Natl. Acad. Sci. USA* **2011**, 108, 2674.
- [45] S. R. Das, Q. Nian, M. Saei, S. Jin, D. Back, P. Kumar, D. B. Janes, M. A. Alam, G. J. Cheng, *ACS Nano* **2015**, 9, 11121.
- [46] a) S. Lee, P. Kumar, Y. Hu, G. J. Cheng, J. Irudayaraj, *Chem. Commun.* **2015**, 51, 15494; b) Y. Hu, S. Lee, P. Kumar, Q. Nian, W. Wang, J. Irudayaraj, G. J. Cheng, *Nanoscale* **2015**, 7, 19885.
- [47] P. Kumar, B. Das, B. Chitara, K. S. Subrahmanyam, K. Gopalakrishnan, S. B. Krupanidhi, C. N. R. Rao, *Macromol. Chem. Phys.* **2012**, 213, 1146.
- [48] a) T. Mueller, F. Xia, P. Avouris, *Nat. Photonics* **2010**, 4, 297; b) X. Cai, A. B. Sushkov, R. J. Suess, M. M. Jadidi, G. S. Jenkins, L. O. Nyakiti, R. L. Myers-Ward, S. Li, J. Yan, D. K. Gaskill, T. E. Murphy, H. D. Drew, M. S. Fuhrer, *Nat. Nanotechnol.* **2014**, 9, 814; c) T.-F. Yeh, J.-M. Syu, C. Cheng, T.-H. Chang, H. Teng, *Adv. Funct. Mater.* **2010**, 20, 2255; d) I. V. Lightcap, T. H. Kosel, P. V. Kamat, *Nano Lett.* **2010**, 10, 577; e) F. Liu, J. Sun, L. Zhu, X. Meng, C. Qi, F.-S. Xiao, *J. Mater. Chem.* **2012**, 22, 5495; f) M. Kitano, D. Yamaguchi, S. Suganuma, K. Nakajima, H. Kato, S. Hayashi, M. Hara, *Langmuir* **2009**, 25, 5068; g) J. Y. S. Kang, J. Chang, *Int. Rev. Chem. Eng.* **2013**, 5, 133; h) K. Nakajima, M. Hara, *ACS Catal.* **2012**, 2, 1296; i) C. Yuan, W. Chen, L. Yan, *J. Mater. Chem.* **2012**, 22, 7456; j) Y. Song, K. Qu, C. Zhao, J. Ren, X. Qu, *Adv. Mater.* **2010**, 22, 2206; k) S. Yang, X. Feng, X. Wang, K. Müllen, *Angew. Chem., Int. Ed.* **2011**, 50, 5339; l) J.-H. Yang, G. Sun, Y. Gao, H. Zhao, P. Tang, J. Tan, A.-H. Lu, D. Ma, *Energy Environ. Sci.* **2013**, 6, 793; m) J. Long, X. Xie, J. Xu, Q. Gu, L. Chen, X. Wang, *ACS Catal.* **2012**, 2, 622; n) M. Yankowitz, S. Chen, H. Polshyn, Y. Zhang, K. Watanabe, T. Taniguchi, D. Graf, A. F. Young, C. R. Dean, *Science* **2019**, 363, 1059; o) Y. Cao, J. Y. Luo, V. Fatemi, S. Fang, J. D. Sanchez-Yamagishi, K. Watanabe, T. Taniguchi, E. Kaxiras, P. Jarillo-Herrero, *Phys. Rev. Lett.* **2016**, 117, 116804; p) K. Kim, A. DaSilva, S. Huang, B. Fallahazad, S. Larentis, T. Taniguchi, K. Watanabe, B. J. LeRoy, A. H. MacDonald, E. Tutuc, *Proc. Natl. Acad. Sci. USA* **2017**, 114, 3364; q) K. Kim, M. Yankowitz, B. Fallahazad, S. Kang, H. C. P. Movva, S. Huang, S. Larentis, C. M. Corbet, T. Taniguchi, K. Watanabe, S. K. Banerjee, B. J. LeRoy, E. Tutuc, *Nano Lett.* **2016**, 16, 1989; r) D. G. Purdie, N. M. Pugno, T. Taniguchi, K. Watanabe, A. C. Ferrari, A. Lombardo, *Nat. Commun.* **2018**, 9, 5387.